An engineered mutant of a host phospholipid synthesis gene inhibits viral replication without compromising host fitness

Received for publication, December 6, 2018, and in revised form, July 16, 2019 Published, Papers in Press, July 30, 2019, DOI 10.1074/jbc.RA118.007051

Guijuan He[‡§1], Zhenlu Zhang[‡§¶1], Preethi Sathanantham[§], Xin Zhang[§], Zujian Wu[‡], Lianhui Xie[‡2], and Xiaofeng Wang[§3]

From the [‡]Fujian Province Key Laboratory of Plant Virology, Institute of Plant Virology, Fujian Agriculture and Forestry University, Fuzhou, Fujian 350002, China, [§]School of Plant and Environmental Sciences, Virginia Tech, Blacksburg, Virginia 24061, and [¶]National Key Laboratory of Crop Biology, National Research Center for Apple Engineering and Technology, College of Horticulture Science and Engineering, Shandong Agricultural University, Tai-An, Shandong 271018, China

Edited by Dennis R. Voelker

Viral infections universally rely on numerous hijacked host factors to be successful. It is therefore possible to control viral infections by manipulating host factors that are critical for viral replication. Given that host genes may play essential roles in certain cellular processes, any successful manipulations for virus control should cause no or mild effects on host fitness. We previously showed that a group of positive-strand RNA viruses enrich phosphatidylcholine (PC) at the sites of viral replication. Specifically, brome mosaic virus (BMV) replication protein 1a interacts with and recruits a PC synthesis enzyme, phosphatidylethanolamine methyltransferase, Cho2p, to the viral replication sites that are assembled on the perinuclear endoplasmic reticulum (ER) membrane. Deletion of the *CHO2* gene inhibited BMV replication by 5-fold; however, it slowed down host cell growth as well. Here, we show that an engineered Cho2p mutant supports general PC synthesis and normal cell growth but blocks BMV replication. This mutant interacts and colocalizes with BMV 1a but prevents BMV 1a from localizing to the perinuclear ER membrane. The mislocalized BMV 1a fails to induce the formation of viral replication complexes. Our study demonstrates an effective antiviral strategy in which a host lipid synthesis gene is engineered to control viral replication without comprising host growth.

Plant viruses are a major threat to stable agronomic production and cause multibillion-dollar losses each year. The planting of virus-resistant cultivars and application of insecticides to control virus-transmitting insects are common practices for controlling viral diseases in the field. However, pesticides cause pollution and leave chemical residue (1) and become ineffective when insects develop resistance. Breeding for crop cultivars with broad-spectrum and stable viral resistance is, therefore, crucial. Conventional breeding has incorporated many available resistance (*R*)[4] genes into elite cultivars to control viral diseases (2–5). *R* genes can be dominant or recessive. Dominant resistance is governed by a specific interaction between an *R* gene and a corresponding avirulence (*Avr*) gene from a pathogen to elicit a hypersensitive response (3, 6). However, there are several issues related to dominant resistance. One is that high mutation rates during viral infection can generate *Avr* gene derivatives that escape recognition and thus overcome the resistance. This is particularly true for RNA viruses whose RNA-dependent RNA polymerases lack proofreading activity. Another issue is strain specificity; although *R* gene products can recognize *Avr* gene products from several virus strains, they are unable to control many other strains (5).

Recessive resistance is usually conferred by a mutated form of a host gene whose WT form encodes a protein that is critical for viral infection (7, 8). Mutants of these genes do not support viral infection but cause no, or only mild, growth phenotypes in virus-resistant plants as the mutants retain their ability to support normal cellular processes. This resistance mechanism is also likely to work in a wide range of crops. For instance, mutated forms of either eukaryotic translation initiation factor 4E (eIF4E) or eIF4(iso)E have been reported as a recessive *R* gene in multiple crops, including barley, lettuce, melon, pepper, pea, and tomato (for a review, see Ref. 9). Additionally, recessive *R* gene–mediated resistance is durable because the mutation rate of host DNA-dependent DNA polymerase is much lower than viral RNA-dependent RNA polymerase (5).

Being the largest among seven viral classes, positive-strand RNA viruses ((+)RNA viruses) include numerous pathogens that infect and cause severe consequences in humans, animals, and plants. Human illness– causing viruses include severe acute respiratory syndrome coronavirus, Zika virus, Dengue virus (DENV), and foot-and-mouth disease virus among many oth-

This work was partially supported by National Science Foundation Grant IOS-1645740 and United States–Israel Binational Agricultural and Research Development Fund Grant US-5019-17. The authors declare that they have no conflicts of interest with the contents of this article.

[1] Supported by a scholarship from the Chinese Scholarship Council.

[2] To whom correspondence may be addressed. Tel.: 86-591-83789439; E-mail: fjxlh@126.com.

[3] To whom correspondence may be addressed. Tel.: 540-231-1868; E-mail: reachxw@vt.edu.

[4] The abbreviations used are: *R*, resistance; *Avr*, avirulence; PC, phosphatidylcholine; BMV, brome mosaic virus; ER, endoplasmic reticulum; eIF4E, eukaryotic translation initiation factor 4E; DENV, Dengue virus; HCV, hepatitis C virus; TBSV, tomato bushy stunt virus; $2a^{pol}$, 2a polymerase; VRC, viral replication complex; FA, fatty acid; PE, phosphatidylethanolamine; PEMT, PE methyltransferase; PMME, monomethyl PE; CDP-DAG, cytidine diphosphodiacylglycerol; SKICH, skeletal muscle– and kidney-enriched inositol phosphatase carboxyl homology carboxyl homology; PS, phosphatidylserine; PI, phosphatidylinositol; PA, phosphatidic acid; IP, immunoprecipitation; nER, perinuclear ER; DAPI, 4′,6-diamidino-2-phenylindole; VHL, von Hippel–Lindau; pAb, polyclonal antibody; ANOVA, analysis of variance.

ers. Importantly, the vast majority of plant viruses are (+)RNA viruses. All (+)RNA viruses have a small genome, encode a limited number of viral proteins, and rely heavily on host factors to achieve a successful infection (10–14). Numerous host factors involved in the replication of hepatitis C virus (HCV) (13, 15, 16), picornavirus (14), brome mosaic virus (BMV) (12, 17), cucumber mosaic virus (18), turnip mosaic virus (10, 19, 20), and tomato bushy stunt virus (TBSV) (11) have been identified and characterized. In theory, loss or mutation of host genes required for viral replication should provide recessive resistance to (+)RNA viruses. It is thus crucial to identify, characterize, and manipulate host genes required for viral replication to develop virus-resistant hosts.

BMV, which serves as a model system to study (+)RNA viruses, is the type member of the Bromoviridae family and a representative member of the alphavirus-like superfamily (21). The genome of BMV is composed of RNA1, RNA2, and RNA3. RNA1 and RNA2 encode replication proteins 1a and 2a polymerase ($2a^{pol}$), respectively (21). RNA3 encodes the movement protein 3a and the coat protein. BMV 1a and $2a^{pol}$ are necessary and sufficient for its replication in barley, its natural host, and in an alternative host, the bakers' yeast *Saccharomyces cerevisiae* (21). BMV replication in yeast cells duplicates nearly all major features of its replication in plant cells (21) and enables systematic screenings of host genes that are involved in viral infection (17). About 100 host genes have been identified to be involved in BMV replication (17), including a group of genes involved in lipid metabolism (22–26). This is consistent with the fact that (+)RNA viruses assemble their viral replication complexes (VRCs) in a tight association with remodeled host intracellular membranes. For example, deleting the *ACB1* gene, which encodes acyl-CoA–binding protein that is involved in the trafficking of long-chain acyl-CoA esters among organelles (27, 28), affects host lipid homeostasis and results in a more than 10-fold decrease in BMV genome replication (22). Additionally, a single point mutation in *OLE1*, which encodes a cellular Δ9 fatty acid desaturase that converts saturated FA to unsaturated FA, causes a mild reduction in host unsaturated FA levels but inhibits BMV RNA replication by 20-fold (23, 24). On the contrary, deleting the *PAH1* gene, which encodes for Pah1p (phosphatidic acid phosphohydrolase) and is the sole yeast ortholog of human *LIPIN* genes, results in a 3-fold increase of BMV replication (26). The requirement of and high sensitivity of viral replication to host lipid composition is a common feature shared by numerous other (+)RNA viruses, including HCV (29, 30), West Nile virus (31), red clover necrotic virus (32), and TBSV (33–35). This highly conserved feature of viral genome replication raises the possibility of developing a novel, durable, and broad-spectrum strategy to control (+)RNA viruses by manipulating host genes involved in lipid metabolism.

Phospholipids are major components of cellular membranes. Phosphatidylcholine (PC) in particular is important as it accounts for up to 50% of the total phospholipids in cells (36). A significant increase in PC levels is associated with the replication of multiple (+)RNA viruses, including DENV (37), flock house virus (38), and poliovirus (39) among others. BMV also significantly increases PC content in yeast and barley cells (25). It was further shown that PC was specifically enriched at the sites of BMV replication (25). PC enrichment at the sites of viral replication was also present in HCV- and poliovirus-infected cells, indicating a conserved feature among a group of (+)RNA viruses (25, 40). In yeast cells, Cho2p (choline-requiring 2), a phosphatidylethanolamine (PE) methyltransferase (PEMT) that converts PE to monomethyl PE (PMME) (41), is recruited to viral replication sites by an interaction with BMV 1a (25). The increase in PC levels and the recruitment of Cho2p to the viral replication sites suggest that the enhanced PC content is synthesized at the sites of BMV replication. Moreover, disrupting PC synthesis by deleting the *CHO2* gene results in a decrease of up to ~80% of BMV RNA synthesis (25), highlighting the critical role of PC in viral replication. However, deleting *CHO2* also disrupts general PC synthesis and thus affects host cell growth (42), preventing the deletion of *CHO2* from being a promising antiviral strategy.

We now report the engineered manipulation of *CHO2* that leads to an inhibition of BMV RNA replication without affecting cell fitness. Specifically, we introduced substitutions in *CHO2* to make the Cho2p-aia mutant in which glycine 102 and glycine 104 were replaced by an alanine residue. The Cho2p-aia functions as well as WT Cho2p in supporting host cell growth and general PC synthesis but does not support BMV RNA replication. We further demonstrate that the Cho2p-aia mutant disrupts the proper localization of BMV 1a and the formation of VRCs. Our data provide a proof of concept for a novel antiviral strategy by manipulating a host lipid metabolism gene to mistarget the viral replication protein away from the proper viral replication sites and prevent the formation of VRCs.

Results

The Cho2p-aia mutant complements the defect of yeast cell growth in cho2Δ cells

The biosynthesis of PC in yeast cells in the absence of exogenous free choline proceeds via the cytidine diphosphodiacylglycerol (CDP-DAG) pathway. Cho2p is a key enzyme in the CDP-DAG pathway where it catalyzes the addition of a methyl moiety to PE to produce PMME (Ref. 41) and Fig. 1*A*). PMME is further converted to PC by Opi3p (overproducer of inositol 3) (Fig. 1*A*), also known as phospholipid methyltransferase (41). Even though deleting *CHO2* inhibits BMV RNA synthesis substantially (25), it also affects host cell growth (25, 42). We set out to identify *CHO2* mutants that disrupt viral replication without affecting host cell growth. To this end, we made various deletions based on structural analysis of Cho2p using Pfam (43) and Protein Homology/Analogy Recognition Engine V2.0 (PHYRE2) (44) programs. Cho2p has two PEMT domains and a skeletal muscle– and kidney-enriched inositol phosphatase carboxyl homology carboxyl homology (SKICH) domain (Fig. 1*B*). We found that the N-terminal 466 amino acids or 365 amino acids of Cho2p (F1 and F2 fragments; Fig. 1*B*), without the second PEMT domain and SKICH domain, were sufficient to support WT level of cell growth. Deleting the first 108 amino acids, however, abolished the ability of F1 to support WT-level cell growth (F3 fragment; Fig. 1*B*). Searching the first 108 amino acids, a putative G*X*G motif (GIG; amino acids 102–104) was identified. The G*X*G motif was reported to play a critical role in

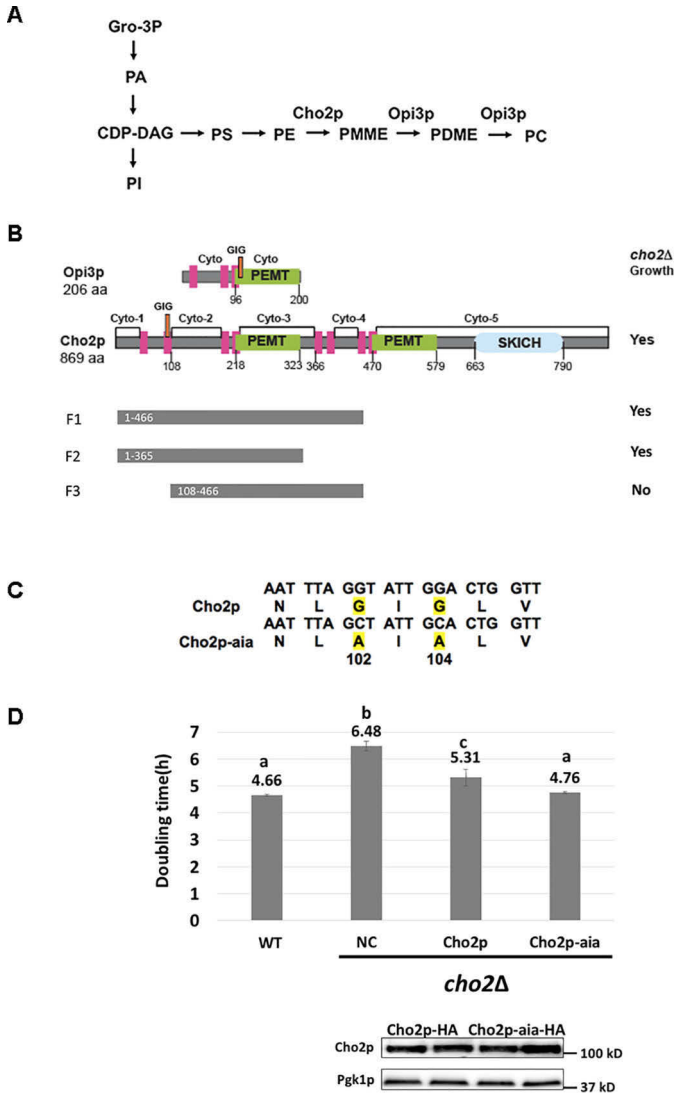

Figure 1. The Cho2p-aia mutant complements the cell growth defect in *cho2*Δ cells. *A*, CDP-DAG pathway for PC biosynthesis in yeast. Cho2p, a PE methyltransferase, catalyzes the addition of a methyl moiety to PE to produce PMME. PMME is subsequently methylated by Opi3p, a phospholipid *N*-methyltransferase, to produce PC. *B*, schematic of Opi3p, Cho2p, and various Cho2p deletion mutants. *C*, nucleic acid and amino acid sequences of amino acids 100–106 of WT Cho2p and Cho2p-aia mutant. Mutated sites are highlighted in *yellow*. *D*, doubling times (hours/generation) of WT cells or *cho2*Δ cells with the expressed Dpm1p, a negative control (*NC*); the WT Cho2p; or the Cho2p-aia mutant. All cells were grown in synthetic defined medium with galactose as the carbon source in the absence of free choline. According to the one-way ANOVA test, means do not differ significantly ($p > 0.05$) if they are indicated with the same *letter*; *error bars* represent S.D. The Western blot shows the accumulation of HA-tagged WT Cho2p or Cho2p-aia in *cho2*Δ cells. Pgk1p served as a loading control.

binding the methyl donor, *N*-adenosylmethionine, to PEMT in human cells (45). We constructed a Cho2p mutant with two alanine substitutions for glycines 102 and 104, referred to as the Cho2p-aia mutant (Fig. 1*C*).

In synthetic defined medium containing galactose as the carbon source without supplemented choline, we found that the doubling time of WT cells was ~4.7 h/generation (Fig. 1*D*). The doubling time of *cho2*Δ cells with the expression of a negative control, an ER-resident protein Dpm1p (dolichol phosphate mannose synthase), was 6.5 h/per generation, which was significantly slower than that of WT cells (Fig. 1*D*, labeled as

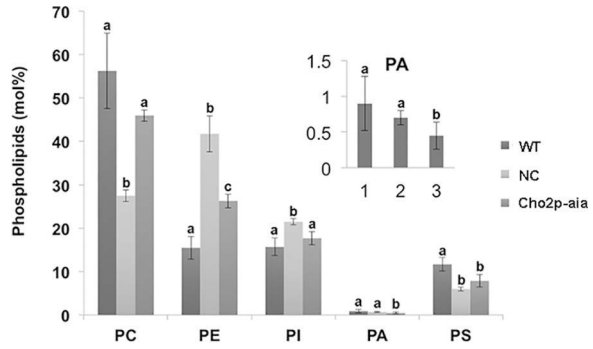

Figure 2. The Cho2p-aia mutant largely restores PC content in *cho2*Δ cells. Phospholipid compositions are expressed as mol % in WT or *cho2*Δ cells expressing *CHO2-aia* or the negative control (*NC*) *DPM1*. According to the one-way ANOVA test, means do not differ significantly ($p > 0.05$) if they are indicated with the same *letter*; *error bars* represent S.D.

NC). The presence of HA-tagged WT Cho2p, nevertheless, improved cell growth and led to a doubling time of 5.3 h/generation (Fig. 1*D*). The presence of Cho2p-aia-HA improved cell growth of *cho2*Δ cells. The doubling time became ~4.8 h/generation, which was similar to that of WT cells. We also confirmed that both HA-tagged WT Cho2p and Cho2p-aia accumulated to similar levels as determined via Western blotting (Fig. 1*D*). Pgk1p (phosphoglycerate kinase) was used as a loading control to show the equal loading of total proteins. We concluded that Cho2p-aia functions as well as WT Cho2p in supporting cell growth (Fig. 1*D*).

The Cho2p-aia mutant largely restores the PC synthesis in cho2Δ cells

The restored growth rate of *cho2*Δ cells in the presence of the Cho2p-aia mutant suggests that Cho2p-aia may function as well as WT Cho2p in supporting PC synthesis. To confirm this assumption, total lipids were extracted from WT and mutant cells and subjected to MS. We quantified phospholipid species by comparing with a defined amount of phospholipid standards and reported the mol % of each of the phospholipid classes in Fig. 2. In *cho2*Δ cells with the expressed negative control Dpm1p (labeled as *NC* in Fig. 2), there was a 2-fold decrease in PC levels compared with WT cells (27% compared with 55%). Expressing *CHO2-aia* in *cho2*Δ cells (*cho2*Δ + Cho2p-aia) increased the percentage of PC levels to 46%, which was significantly higher than that of negative control ($p < 0.05$) and not statistically significantly different from that in WT cells. The levels (21%) of phosphatidylinositol (PI) in *cho2*Δ cells were significantly higher than those of WT (16%). The expressed Cho2p-aia largely restored the PI levels to 17%, which is not significantly different from the WT levels (Fig. 2). For PE, which is the substrate of PC, deleting *CHO2* had a dramatic effect as PE levels increased to 42% of total phospholipids from the 16% in WT cells. Expressing *CHO2-aia* partially restored PE levels because it decreased PE levels to 27%, which was significantly lower from that measured in cells lacking *CHO2* but still higher than WT levels (Fig. 2, comparing *NC* and *Wt*). Similarly, decreased levels of phosphatidylserine (PS) was not restored to WT levels when Cho2p-aia was expressed in *cho2*Δ cells. Moreover, there was a significant decrease in phosphatidic acid (PA) levels in the presence of Cho2p-aia over the WT levels.

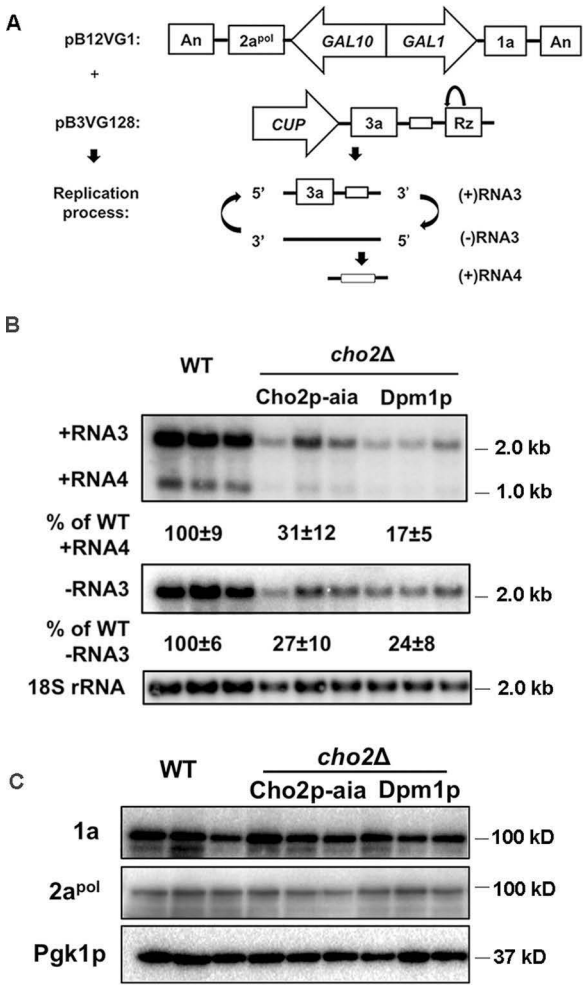

Figure 3. The Cho2p-aia mutant fails to rescue the BMV replication defect in *cho2*Δ cells. *A*, diagram of BMV replication process in yeast. BMV 1a and $2a^{pol}$ were expressed from plasmid pB12VG1 under the control of the *GAL1* and *GAL10* promoters, respectively. BMV RNA3 was launched from plasmid pB3VG128 under the control of the copper-inducible *CUP1* promoter, but no copper was added to the growth media. *B*, BMV replication in WT cells or in *cho2*Δ cells with the expressed Dpm1p or Cho2p-aia. BMV positive- and negative-strand RNAs were detected by ^{32}P-labeled BMV strand-specific probes. 18S rRNA served as a loading control. The blot detecting (−)RNA3 was exposed for a longer time than that of (+)RNAs. *C*, BMV 1a and $2a^{pol}$ accumulation in WT cells or in *cho2*Δ cells with the expressed Cho2p-aia or Dpm1p. Pgk1p served as a loading control.

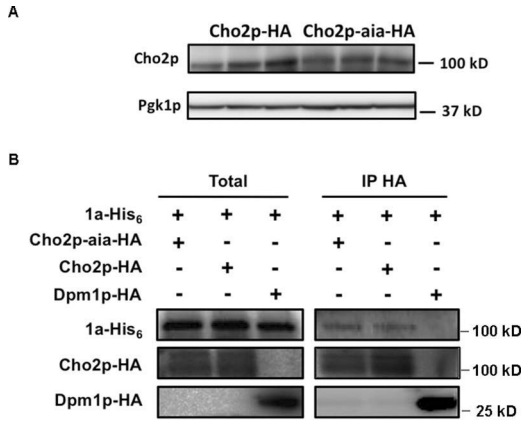

Figure 4. The Cho2p-aia mutant interacts with BMV 1a. *A*, Western blot showing the accumulation of HA-tagged Cho2p-aia or WT Cho2p in *cho2*Δ cells with the presence of BMV components. Pgk1p served as a loading control. *B*, coimmunoprecipitation of Cho2p-aia-HA and BMV 1a-His_6. Cell lysates were subjected to immunoprecipitation using an anti-HA (*IP HA*) pAb followed by Western blotting with an anti-His_6 mAb or anti-HA pAb. WT Cho2p served as a positive control, and Dpm1p served as a negative control.

Reasons for the decrease of PA levels and the partial restoration of alterations in PE and PS levels by Cho2p-aia are not clear. Nevertheless, our data suggest that Cho2p-aia is able to largely restore general PC synthesis for cell growth. Our data also indicate that cell growth is not noticeably affected by the moderate differences in phospholipid composition (Figs. 1 and 2).

The Cho2p-aia mutant fails to rescue the BMV replication defect in cho2Δ cells

Given that the Cho2p-aia mutant supported WT-level cell growth and largely restored PC content to WT levels in *cho2*Δ cells, we next checked whether Cho2p-aia is able to complement the viral RNA replication defect. In the engineered BMV yeast system (46), BMV 1a, $2a^{pol}$, and RNA3 are expressed from plasmids to provide the necessary components required for BMV RNA replication (Fig. 3*A*). In WT yeast cells, negative-strand RNA3 and positive-strand RNA4 were detected using BMV RNA strand–specific probes, indicating full replication (Fig. 3*B*). In *cho2*Δ cells with the expressed Dpm1p, which is not known to be involved in BMV replication and is used as a negative control, accumulated positive-strand RNA4 and negative-strand RNA3 were about 17 and 24% of WT levels, respectively. Expressing *CHO2-aia* did not improve BMV replication as positive-strand RNA4 and negative-strand RNA3 levels were similar to those in *cho2*Δ cells expressing *DPM1* (Fig. 3*B*), indicating that Cho2p-aia failed to complement the BMV replication defect in *cho2*Δ cells.

To identify specific reasons why BMV replication defects were not complemented by Cho2p-aia, we first checked the accumulation of BMV 1a and $2a^{pol}$, which are necessary and sufficient for BMV replication. As shown in Fig. 3*C*, there was no significant difference in accumulated levels of 1a and $2a^{pol}$ in these cells, ruling out the possibility that the inhibited BMV genome replication was due to negative effects on expression and/or stability of the viral replication proteins.

The Cho2p-aia mutant interacts with BMV 1a

Because the Cho2p-aia mutant failed to complement the defective BMV RNA synthesis, we wanted to confirm whether Cho2p-aia was stably expressed during viral replication. Western blotting determined that levels of HA-tagged Cho2p-aia and WT Cho2p were similar (Fig. 4*A*), indicating that Cho2p-aia-HA is stably expressed and accumulates in the absence (Fig. 1*D*) or presence (Fig. 4*A*) of BMV replication.

Cho2p interacts with and is recruited by BMV 1a to the sites of viral replication to facilitate BMV genome replication (25). It is possible that Cho2p-aia fails to interact with 1a and therefore is not recruited to the VRCs. To confirm or reject this notion, we performed a coimmunoprecipitation (co-IP) assay by coexpressing HA-tagged Cho2p, Cho2p-aia, or Dpm1p with His_6-tagged 1a in yeast cells. Similar to Fig. 4*A*, Cho2p-HA and

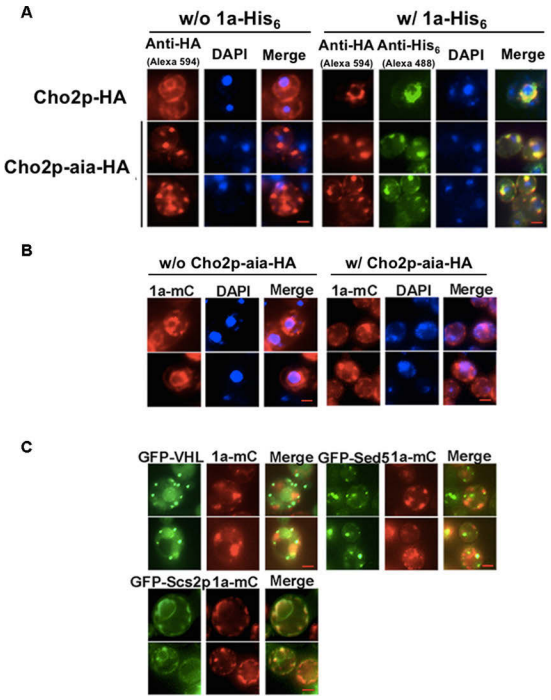

Figure 5. BMV 1a mislocalizes in the presence of Cho2p-aia. *A*, microscopy images showing the distribution patterns of Cho2p-HA and Cho2p-aia-HA in *cho2*Δ cells in the absence (*w/o*) or presence (*w/*) of BMV 1a-His$_6$. Cho2p-HA and Cho2p-aia-HA were detected using an anti-HA pAb and a secondary antibody conjugated to Alexa Fluor 594. BMV 1a was detected using an anti-His$_6$ mAb and a secondary antibody conjugated to Alexa Fluor 488. *B*, distribution patterns of BMV 1a-mCherry in *cho2*Δ cells in the absence or presence of Cho2p-aia-HA. *C*, distribution pattern of BMV 1a-mCherry in *cho2*Δ cells in the presence of Cho2p-aia-HA and GFP-tagged organelle markers for inclusion bodies (VHL), Golgi (Sed5p), or ER membrane (Scs2p). Nuclei were stained with DAPI, and *scale bars* are 2.5 μm in all panels.

Cho2p-aia-HA accumulated to similar levels in the presence of BMV 1a (Fig. 4*B*, *Total*). As expected from our previous work, precipitating Cho2p-HA with anti-HA antibody pulled down 1a-His$_6$ (Ref. 25 and Fig. 4*B*). On the contrary, 1a-His$_6$ was not coprecipitated with Dpm1p-HA, which was used as a negative control and is not expected to interact with BMV 1a (25). To our surprise, 1a-His$_6$ was also pulled down along with Cho2p-aia-HA (Fig. 4*B*), indicating that Cho2p-aia-HA is still associated or interacts with BMV 1a.

Cho2p-aia prevents the localization of BMV 1a at the perinuclear ER membrane

BMV 1a is associated with the perinuclear ER (nER) membrane where it invaginates the outer nER membrane to form VRCs (12). BMV 1a recruits host proteins such as reticulon homology proteins (47), Snf7 (sucrose non-fermenting 7) (48), and Cho2p (25) to assemble functional VRCs. Like the majority of lipid enzymes, Cho2p is normally localized in ER membranes where lipids are synthesized. In agreement with our previous results (25) and as shown in Fig. 5*A*, Cho2p-HA was detected by immunofluorescence microscopy and appeared as a two-ring localization pattern in 43.1% of cells (n = 153). The larger ring represents peripheral ER membranes, and the smaller ring surrounding the DAPI-stained nucleus corresponds to the nER membrane (Fig. 5*A*, *upper left panels*). In the presence of 1a, Cho2p is depleted from peripheral ER membranes, enriched in the nER membrane, and colocalized with 1a-His$_6$ (59 of a total of 178 cells) (Fig. 5*A*, *upper right panels*).

To determine whether Cho2p-aia can be relocalized by 1a, we first expressed HA-tagged Cho2p-aia in the absence of BMV replication in *cho2*Δ cells and tested its distribution. To our surprise, among all cells (n = 326) in which we can detect Cho2p-aia-HA, only ~6 of the total 326 cells (1.8%) had a two-ring distribution pattern, and in sharp contrast, Cho2p-aia-HA was found as puncta in about 72% of cells (Fig. 5*A*, *lower left panels*). Intriguingly, when Cho2p-aia-HA and 1a-His$_6$ were expressed simultaneously, the localization of 1a was altered. BMV 1a-His$_6$ was localized to the nER membrane in only ~3.7% cells (12 of 328 cells) but as puncta in 73.2% cells where we can clearly detect signals of 1a-His$_6$, Cho2p-aia-HA, and DAPI (Fig. 5*A*, *lower right panels*). It should be noted that even though localization patterns of both Cho2p-aia and 1a changed, they colocalized with each other in all cells where both can be detected, consistent with our co-IP results that Cho2p-aia is associated or interacts with 1a (Fig. 4*B*).

To better and easily characterize the nature of punctate structures of BMV 1a in the presence of Cho2p-aia, we used an mCherry-tagged 1a, which we have previously shown to have a similar localization pattern as that of 1a-His$_6$ in WT cells (49). In *cho2*Δ cells, about 35.5% of cells (n = 262) expressing 1a-mCherry have a ring structure in the nER membrane (Fig. 5*B*, *left panel*) similar to that in WT cells (25, 49). The distribution pattern of 1a-mCherry was also similar to that of 1a-His$_6$ in the presence of Cho2p-aia as it was associated with punctate structures in 74.6% (n = 386) of cells (Fig. 5, *A* and *B*). To determine whether BMV 1a was being redistributed to a different membrane in the presence of Cho2p-aia, we coexpressed 1a-mCherry, Cho2p-aia, and GFP-tagged organelle markers. By comparing 1a-mCherry distributions with those of organelle markers, we found that the majority of puncta did not colocalize with the inclusion body marker von Hippel–Lindau (VHL) (50) or the Golgi marker Sed5p (suppressor of Erd2 deletion 5) (51) (Fig. 5*C*). In contrast, these dots were colocalized with the ER marker Scs2p (suppressor of choline sensitivity 2) (52) in peripheral ER membranes in about 49% of cells that we counted (n = 123), and only 2.3% of cells have 1a-mCherry localized in the nER membrane (Fig. 5*C*). Taken together, our results indicate that Cho2p-aia disrupts the normal distribution of 1a to the nER membrane; however, 1a is still primarily associated with ER membranes.

The Cho2p-aia mutant prevents the formation of BMV VRCs

BMV 1a invaginates the outer nER membrane into the lumen to form spherular VRCs during BMV replication (12, 53). These spherular compartments are about 60–80 nm in diameter with an ~10-nm neck connecting to the cytoplasm (53, 54). The abundance and size of these VRCs can change significantly with deletion or mutation of host genes involved in membrane shaping or lipid metabolism (22, 47, 48). We previously reported that, in *cho2*Δ cells, 1a was detected at the nER membrane, and spherular VRCs were formed, but they were larger than those in WT cells and were not functional in genome replication (25). Because the expressed Cho2p-aia affected 1a's association with

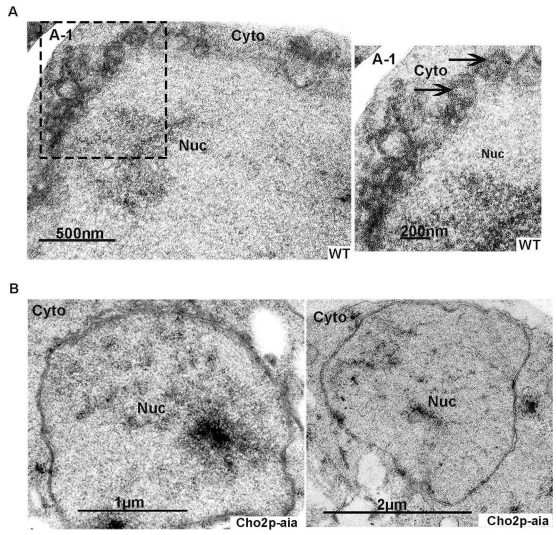

Figure 6. The Cho2p-aia mutant affects the formation of BMV replication complexes. *A*, electron micrographs of VRCs formed in WT cells in the presence of all BMV replication components. Image *A-1* is a higher magnification of the *boxed* area from the image on the *left*. *Black arrows* in *A-1* point to VRCs. The spherular VRCs were observed in 11 of 67 cells. *B*, electron micrographs of *cho2*Δ cells with the expressed Cho2p-aia in the presence of all BMV replication components. 100 cells with clear nuclear membranes were recorded. *Nuc*, nucleus; *Cyto*, cytoplasm.

the nER membrane (Fig. 5), we predicted that VRC formation could be affected. To confirm this, we checked the formation of VRCs by transmission EM in WT cells or *cho2*Δ cells expressing *CHO2-aia* in the presence of 1a, $2a^{pol}$, and RNA3. In WT cells with BMV components, the percentage of cells with spherular VRCs was ~16% (11 of 67 cells). The average number of spherules was 6 (S.D. = 1.8) with an average diameter of 65 ± 8 nm (Fig. 6*A*). However, among the 100 cells checked, no spherical structures were observed in *cho2*Δ cells expressing the BMV replication components and Cho2p-aia. Of note, the inner and outer nER membranes were clearly observed in these cells (Fig. 6*B*). The failure to identify spherular VRCs is consistent with our results that Cho2p-aia inhibited the proper targeting of BMV 1a to the nER membrane in *cho2*Δ cells (Fig. 5).

Discussion

Positive-strand RNA viruses have limited protein-coding capacity and replicate in a tight association with host intracellular membranes to form the viral replication complexes. As major components of cellular membranes, lipids play critical roles in the replication of multiple (+)RNA viruses (55–58). For example, PI4P plays a key role in the replication of multiple (+)RNA viruses, including HCV (29, 30, 59–61) and enteroviruses (29). Poliovirus and several enteroviruses promote an enrichment of free cholesterol to the sites of their replication (62, 63). Disrupting sterol biosynthesis and composition inhibits the replication of West Nile virus and DENV (64, 65). Among plant viruses, red clover necrotic mosaic virus promotes PA production by hijacking phospholipase D to the sites of its replication (32). TBSV and carnation Italian ringspot virus transport PE to viral replication sites to build the PE-enriched VRCs for their replication (33, 66). For BMV, whose replication also requires balanced lipid homeostasis, phospholipids PC and PA are particularly important (22–26). Thus, dissecting the role of phospholipids in BMV replication and, in turn, manipulating phospholipid metabolism may potentially provide antiviral strategies with a broad range and durable resistance. A major challenge for engineering lipid synthesis genes to control viruses and other pathogens, however, is that lipids also play crucial roles in cellular processes. Any manipulation of lipid synthesis genes will potentially affect host growth. Here, we generated a mutant, Cho2p-aia, which largely complemented PC synthesis and host growth defects but failed to support BMV replication (Figs. 1–3). Although the Cho2p-aia mutant still interacted with BMV 1a (Fig. 4), it disrupted the normal distribution of BMV 1a (Fig. 5) and thus affected the formation of BMV VRCs (Fig. 6).

All well-studied (+)RNA viruses assemble their VRCs in association with various organelle membranes. As such, the trafficking of viral replication proteins to their destination organelles is the first and a critical step for VRC formation. Without transmembrane domains, BMV 1a is associated with the nER membrane via an amphipathic α-helix domain, helix A (67, 68). Mutations in helix A result in two major phenotypes: 1a either no longer localizes to the nER, or it induces the formation of smaller, abundant, nonfunctional VRCs compared with WT 1a (69). Besides 1a's helix A domain, host genes also regulate 1a's distribution. For example, coat protein complex II vesicle cargo receptor Erv14p (ER-vesicle protein of 14 kDa) is required for targeting 1a to the nER membrane (49). In cells lacking *ERV14*, 1a no longer associates with the nER membrane but is distributed in punctate dots and large clusters that are located at peripheral ER membranes (49). However, the mechanism by which Erv14p and coat protein complex II vesicles regulate 1a's localization remains unclear. Expressing *CHO2-aia* resulted in a similar phenotype as the majority of 1a localized in peripheral ER–associated punctate dots (Fig. 5). It is unclear whether the punctate structures present in *erv14*Δ cells or cells with the Cho2p-aia mutant are related or formed in a similar fashion.

It should be noted that 1a interacts (Fig. 4*B*) and completely colocalizes with the Cho2p-aia mutant in puncta (Fig. 5*A*). Because Cho2p-aia interacts with 1a and localizes to punctate structures when expressed alone, it is most likely that Cho2p-aia recruits 1a to these dot structures. If this is the case, it is contrary to WT Cho2p, which is recruited to the nER membrane–localized viral replication sites by 1a via their interaction (Fig. 5*A* and Ref. 25). Alternatively, although Cho2p-aia largely complemented PC defects in *cho2*Δ cells, the phospholipid composition was not identical to that in WT cells: levels of PE were significantly higher and levels of PA and PS were lower than WT levels (Fig. 2). These lipid compositional changes might affect the physical properties of membranes, including thickness, intrinsic curvature, and fluidity. Such changes may affect membrane fusion and fission or the conformation of membrane-associated/integral proteins (70–72), including ER membrane–localized Cho2p-aia and 1a. It is also remotely possible that both 1a and Cho2p-aia are similarly affected and targeted to punctate structures independently. However, the localization of another ER-resident protein, Scs2p, was not affected, and a two-ring localization pattern was still observed

in the presence of Cho2p-aia (Fig. 5*C*), arguing against a similar effect on conformation and/or localization of all ER membrane proteins. Cho2p is involved in converting PE to PC. In the presence of Cho2p-aia, we observed close-to-WT levels of PC, but PE contents were still significantly higher than WT levels (Fig. 2). PE is primarily synthesized by phosphatidylserine decarboxylase from PS in mitochondria and then transported to ER membranes where PE is methylated first by Cho2p (41). It is possible that the mislocalization of Cho2p-aia from entire ER membranes to puncta may affect the access of PE by Cho2p-aia and as such leads to enhanced levels of PE compared with WT levels.

All (+)RNA viruses depend entirely on host factors such as proteins or lipids to complete their life cycles. In theory, host genes required for viral infection (also termed susceptibility genes) (73) can be potentially targeted to develop viral resistance, similar to recessive *R* genes in nature. The following are some advantages of engineering host genes to achieve virus resistance. 1) Viral resistance caused by the loss of or mutation(s) of a host gene is durable because host genes are less likely to mutate than viral genes under infections. 2) Multiple genes can be targeted in combination to achieve a better or complete control of viral infection. 3) The same or similar manipulation of a specific gene can be applied to several crops. However, these host genes may play critical roles in cellular processes, and in turn, alterations of such host genes may lead to side effects on host survival. This is true for *CHO2*, whose deletion inhibited BMV replication more than 5-fold but also caused host cell growth defects (Ref. 25 and Figs. 1–3). However, cells expressing *CHO2-aia* grew as well as WT cells but still inhibited BMV replication by ~5-fold. This provides proof-of-principle evidence that host lipid genes can be engineered to control (+)RNA virus genome replication without compromising host fitness. We note that the deletion of or mutations in *CHO2* substantially inhibited but did not eliminate BMV replication, suggesting that BMV may acquire PC through the Kennedy pathway, which is a secondary PC synthesis pathway in yeast but the primary pathway in higher eukaryotes. In addition to manipulating *CHO2*, targeting another component(s) of the Kennedy pathway or other related processes coordinately may provide complete blockage of BMV replication.

In summary, we identified a *CHO2* mutant, Cho2p-aia, that supports general PC synthesis required for cell growth but fails to support BMV replication. The Cho2p-aia mutant prevented BMV replication protein 1a from localizing to the perinuclear ER membrane and as such blocked the formation of VRCs and inhibited viral replication. This indicates that engineering host lipid synthesis genes can be an effective way of controlling viral replication without compromising host fitness.

Experimental procedures

Yeast strains and growth conditions

The *Saccharomyces cerevisiae* strain YPH500 (*MATα ura3–52, lys2–801, ade2–101, trp1-Δ63, his3-Δ200, leu2-Δ1*) and YPH500-based *CHO2* deletion mutant (25) were used in all experiments. Yeast cells were grown at 30 °C in synthetic defined medium containing 2% galactose as the carbon source. Histidine, leucine, uracil, or combinations of them were omitted from the medium to maintain selection for different plasmid combinations. After two passages (36–48 h) in synthetic defined medium, cells were harvested when the optical density at 600 nm (OD_{600}) reached between 0.4 and 1.0. The doubling time was calculated using the following equation: (Hours cells grown × ln(2))/ln(Final OD_{600}/Initial OD_{600}).

Plasmids

To launch BMV replication, plasmid pB12VG1 expressing BMV 1a and $2a^{pol}$ and plasmid pB3VG128 transcribing BMV RNA3 were used (49). His_6- or mCherry-tagged BMV 1a was expressed under the control of the *GAL1* promoter from pB1YT3-cH6 or pB1YT3-mC, respectively. G102A and G104A mutations were introduced into *CHO2* by an overlapping PCR-based approach using a pair of primers, 5′-GTAATGCAGAACCAGTgCAATAgCTAAATTATAAGCAATTCTCCA-3′ and 5′-TGGAGAATTGCTTATAATTTAGcTATTGcACTGGTTCTGCATTAC-3′. (nucleic acids in lowercase were intended to introduce mutations). Both Cho2p-HA and Cho2p-aia-HA were expressed under the control of the *GAL1* promoter from a centromeric plasmid. Plasmids expressing organelle markers, GFP-VHL, GFP-Scs2, and GFP-Sed5, were provided by Dr. Maya Schuldiner (Weizmann Institute of Sciences, Israel).

Lipid analysis

Ten OD_{600} units of yeast cells were harvested, and total lipids were extracted as described previously (74). Total lipids were reconstituted in chloroform:methanol:water (65:35:8, v/v/v; 500 ul) with the addition of the phospholipid internal standard mixture purchased from Kansas Lipidomics Research Center. The phospholipid compositions were analyzed by a Waters I-class UPLC interfaced with a Waters Synapt G2-S mass spectrometer (Waters) using conditions as described (75). Data normalization to the internal standards for mol % calculations was performed as described previously (76).

RNA extraction and Northern blotting

Yeast cells were harvested, and total RNA was extracted by a hot phenol method (77). Equal amounts of total RNA were prepared for Northern blot analysis. ^{32}P-Labeled probes specific to BMV positive- or negative-strand RNAs or 18S rRNA were used for the hybridization. 18S rRNA was used as a loading control to eliminate loading variations. Radioactive signals of BMV positive-, negative-strand, or 18S rRNA were scanned using a Typhoon FLA 7000 phosphoimaging system, and the intensity of signals was quantified using ImageQuant TL software (GE Healthcare).

Protein extraction and Western blotting

Two OD_{600} units of yeast cells were harvested, and total proteins were extracted as described previously (49). Equal volumes of total proteins were analyzed using SDS-PAGE and transferred to a polyvinylidene difluoride membrane. Rabbit

anti-BMV 1a antiserum (1:10,000 dilution; a gift from Dr. Paul Ahlquist at the University of Wisconsin-Madison), mouse anti-BMV $2a^{Pol}$ (1:3,000 dilution), rabbit anti-HA (1:3,000 dilution; Thermo Fisher Scientific, catalog number 71-5500), mouse anti-His (1:3,000 dilution; Genscript, catalog number A00186), mouse anti-Pgk1 (1:10,000 dilution; Thermo Fisher Scientific, catalog number 459250), or mouse anti-Dpm1p (1:3,000 dilution; Thermo Fisher Scientific, catalog number A6429) was used as the primary antibody; horseradish peroxidase–conjugated anti-rabbit or anti-mouse antibody (1:10,000 dilution; Thermo Fisher Scientific, catalog numbers 32460 and 32430) together with the Supersignal West Femto substrate (Thermo Scientific Thermo Fisher Scientific, catalog number 32460) was used to detect target proteins.

Coimmunoprecipitation assay

Ten OD_{600} units of yeast cells were harvested, and the co-IP assay was performed as described previously (49). Briefly, harvested cells were lysed in radioimmunoprecipitation assay buffer (50 mM Tris at pH 8.0, 1% Nonidet P-40, 0.1% SDS, 150 mM NaCl, 0.5% sodium deoxycholate, 5 mM EDTA, 10 mM NaF, 10 mM $NaPP_i$, and protease inhibitor mixture). Cell debris was removed, and the supernatant was mixed with Protein A–Sepharose beads and anti-HA pAb overnight at 4 °C. Beads were washed three times with radioimmunoprecipitation assay buffer, resuspended in 1× SDS gel-loading buffer, and boiled for 10 min. Samples were resolved by SDS-PAGE followed by Western blotting with anti-His_6 mAb and anti-HA pAb to detect target proteins.

Immunofluorescence assay

Two OD_{600} units of yeast cells were harvested and fixed with 4% (v/v) formaldehyde for 30 min at 30 °C. After removing the cell wall using lyticase, spheroplasts were permeabilized with 0.1% Triton X-100 and incubated with specified primary antibodies (anti-His_6 mAb or anti-HA pAb at 1:100 dilution) overnight at 4 °C followed by an incubation with secondary antibodies (1:100 dilution) for 1 h at room temperature. Secondary antibodies were Alexa Fluor 488–conjugated anti-mouse (Thermo Fisher Scientific, catalog number A11001) and Alexa Fluor 594–conjugated anti-rabbit antibodies (Jackson ImmunoResearch Laboratories, catalog number 711-545-152). The nucleus was stained with DAPI (Vector Laboratories, catalog number H-1200) for 10 min. Images were captured using a Zeiss epifluorescence microscope at the Fralin microscopy facility, Virginia Tech.

EM

Ten OD_{600} units of yeast cells were harvested. Fixation, dehydration, and embedding were performed as described previously (25). Images were captured using a JEOL JEM 1400 transmission electron microscope at the Virginia–Maryland College of Veterinary Medicine, Virginia Tech.

Statistical analysis

One-way ANOVA analysis was used to compare phospholipids or doubling time in WT and mutant cells. Error bars represent the standard deviation.

Author contributions—G. H., Z. Z., P. S., and X. Z. data curation; G. H. and Z. Z. formal analysis; G. H. and X. W. writing-original draft; G. H. project administration; Z. Z., P. S., and X. Z. methodology; Z. W., L. X., and X. W. supervision; Z. W. and L. X. funding acquisition; X. W. writing-review and editing.

Acknowledgments—We thank Haijie Liu, Jianhui Li, Nicholas Todd, and Elizabeth Barton for general help and assistance. We appreciate help from Kathy Lowe at the Virginia-Maryland College of Veterinary Medicine, Virginia Tech (VT) for EM work, Dr. Kristi DeCourcy at the Fralin Life Science Institute, VT for fluorescence microscopy work, and Drs. Sherry Hildreth and Richard Helm at the Mass Spectrometry Incubator, VT for measuring phospholipids. We are grateful to Drs. George Carman, Arturo Diaz, and Janet Webster for critical reading of our manuscript.

References

1. Pimentel, D. (2005) Environmental and economic costs of the application of pesticides primarily in the United States. *Environ. Dev. Sustain.* **7,** 229–252 CrossRef
2. Dangl, J. L., and Jones, J. D. (2001) Plant pathogens and integrated defence responses to infection. *Nature* **411,** 826–833 CrossRef Medline
3. Kang, B. C., Yeam, I., and Jahn, M. M. (2005) Genetics of plant virus resistance. *Annu. Rev. Phytopathol.* **43,** 581–621 CrossRef Medline
4. Maule, A. J., Caranta, C., and Boulton, M. I. (2007) Sources of natural resistance to plant viruses: status and prospects. *Mol. Plant Pathol.* **8,** 223–231 CrossRef Medline
5. Galvez, L. C., Banerjee, J., Pinar, H., and Mitra, A. (2014) Engineered plant virus resistance. *Plant Sci.* **228,** 11–25 CrossRef Medline
6. Martin, G. B., Bogdanove, A. J., and Sessa, G. (2003) Understanding the functions of plant disease resistance proteins. *Annu. Rev. Plant Biol.* **54,** 23–61 CrossRef Medline
7. Hashimoto, M., Neriya, Y., Yamaji, Y., and Namba, S. (2016) Recessive resistance to plant viruses: potential resistance genes beyond translation initiation factors. *Front. Microbiol.* **7,** 1695 CrossRef Medline
8. Truniger, V., and Aranda, M. A. (2009) Recessive resistance to plant viruses. *Adv. Virus Res.* **75,** 119–159 CrossRef Medline
9. Wang, A., and Krishnaswamy, S. (2012) Eukaryotic translation initiation factor 4E mediated recessive resistance to plant viruses and its utility in crop improvement. *Mol. Plant Pathol.* **13,** 795–803 CrossRef Medline
10. Wang, A. (2015) Dissecting the molecular network of virus-plant interactions: the complex roles of host factors. *Annu. Rev. Phytopathol.* **53,** 45–66 CrossRef Medline
11. Nagy, P. D. (2016) Tombusvirus-host interactions: co-opted evolutionarily conserved host factors take center court. *Annu. Rev. Virol.* **3,** 491–515 CrossRef Medline
12. Diaz, A., and Wang, X. (2014) Bromovirus-induced remodeling of host membranes during viral RNA replication. *Curr. Opin. Virol.* **9,** 104–110 CrossRef Medline
13. Belov, G. A., and van Kuppeveld, F. J. (2012) (+)RNA viruses rewire cellular pathways to build replication organelles. *Curr. Opin. Virol.* **2,** 740–747 CrossRef Medline
14. Belov, G. A. (2014) Modulation of lipid synthesis and trafficking pathways by picornaviruses. *Curr. Opin. Virol.* **9,** 19–23 CrossRef Medline
15. Randall, G., Panis, M., Cooper, J. D., Tellinghuisen, T. L., Sukhodolets, K. E., Pfeffer, S., Landthaler, M., Landgraf, P., Kan, S., Lindenbach, B. D., Chien, M., Weir, D. B., Russo, J. J., Ju, J., Brownstein, M. J., *et al.* (2007) Cellular cofactors affecting hepatitis C virus infection and replication. *Proc. Natl. Acad. Sci. U.S.A.* **104,** 12884–12889 CrossRef Medline
16. Paul, D., Madan, V., and Bartenschlager, R. (2014) Hepatitis C virus RNA replication and assembly: living on the fat of the land. *Cell Host Microbe* **16,** 569–579 CrossRef Medline
17. Kushner, D. B., Lindenbach, B. D., Grdzelishvili, V. Z., Noueiry, A. O., Paul, S. M., and Ahlquist, P. (2003) Systematic, genome-wide identifica-

tion of host genes affecting replication of a positive-strand RNA virus. *Proc. Natl. Acad. Sci. U.S.A.* **100,** 15764–15769 CrossRef Medline
18. Guo, Z., Lu, J., Wang, X., Zhan, B., Li, W., and Ding, S. W. (2017) Lipid flippases promote antiviral silencing and the biogenesis of viral and host siRNAs in Arabidopsis. *Proc. Natl. Acad. Sci. U.S.A.* **114,** 1377–1382 CrossRef Medline
19. Li, F., Zhang, C., Li, Y., Wu, G., Hou, X., Zhou, X., and Wang, A. (2018) Beclin1 restricts RNA virus infection in plants through suppression and degradation of the viral polymerase. *Nat. Commun.* **9,** 1268 CrossRef Medline
20. Jiang, J., Patarroyo, C., Garcia Cabanillas, D., Zheng, H., and Laliberté, J. F. (2015) The vesicle-forming 6K2 protein of turnip mosaic virus interacts with the COPII coatomer Sec24a for viral systemic infection. *J. Virol.* **89,** 6695–6710 CrossRef Medline
21. Wang, X., and Ahlquist, P. (2008) Brome mosaic virus (Bromoviridae), in *Encyclopedia of Virology* (Mahy, B. W. J., and van Regenmortel, M. H. V., eds) 3rd Ed., pp. 381–386, Elsevier, New York
22. Zhang, J., Diaz, A., Mao, L., Ahlquist, P., and Wang, X. (2012) Host acyl-CoA binding protein regulates replication complex assembly and activity of a positive-strand RNA virus. *J. Virol.* **86,** 5110–5121 CrossRef Medline
23. Lee, W. M., Ishikawa, M., and Ahlquist, P. (2001) Mutation of host Δ9 fatty acid desaturase inhibits brome mosaic virus RNA replication between template recognition and RNA synthesis. *J. Virol.* **75,** 2097–2106 CrossRef Medline
24. Lee, W. M., and Ahlquist, P. (2003) Membrane synthesis, specific lipid requirements, and localized lipid composition changes associated with a positive-strand RNA virus RNA replication protein. *J. Virol.* **77,** 12819–12828 CrossRef Medline
25. Zhang, J., Zhang, Z., Chukkapalli, V., Nchoutmboube, J. A., Li, J., Randall, G., Belov, G. A., and Wang, X. (2016) Positive-strand RNA viruses stimulate host phosphatidylcholine synthesis at viral replication sites. *Proc. Natl. Acad. Sci. U.S.A.* **113,** E1064–E1073 CrossRef Medline
26. Zhang, Z., He, G., Han, G. S., Zhang, J., Catanzaro, N., Diaz, A., Wu, Z., Carman, G. M., Xie, L., and Wang, X. (2018) Host Pah1p phosphatidate phosphatase limits viral replication by regulating phospholipid synthesis. *PLoS Pathog.* **14,** e1006988 CrossRef Medline
27. Du, Z. Y., Arias, T., Meng, W., and Chye, M. L. (2016) Plant acyl-CoA-binding proteins: an emerging family involved in plant development and stress responses. *Prog. Lipid Res.* **63,** 165–181 CrossRef Medline
28. Neess, D., Bek, S., Engelsby, H., Gallego, S. F., and Færgeman, N. J. (2015) Long-chain acyl-CoA esters in metabolism and signaling: role of acyl-CoA binding proteins. *Prog. Lipid Res.* **59,** 1–25 CrossRef Medline
29. Hsu, N. Y., Ilnytska, O., Belov, G., Santiana, M., Chen, Y. H., Takvorian, P. M., Pau, C., van der Schaar, H., Kaushik-Basu, N., Balla, T., Cameron, C. E., Ehrenfeld, E., van Kuppeveld, F. J., and Altan-Bonnet, N. (2010) Viral reorganization of the secretory pathway generates distinct organelles for RNA replication. *Cell* **141,** 799–811 CrossRef Medline
30. Berger, K. L., Cooper, J. D., Heaton, N. S., Yoon, R., Oakland, T. E., Jordan, T. X., Mateu, G., Grakoui., A, and Randall, G. (2009) Roles for endocytic trafficking and phosphatidylinositol 4-kinase III alpha in hepatitis C virus replication. *Proc. Natl. Acad. Sci. U.S.A.* **106,** 7577–7582 CrossRef Medline
31. Martín-Acebes, M. A., Blázquez, A. B., Jiménez de Oya, N., Escribano-Romero, E., and Saiz, J. C. (2011) West Nile virus replication requires fatty acid synthesis but is independent on phosphatidylinositol-4-phosphate lipids. *PLoS One* **6,** e24970 CrossRef Medline
32. Hyodo, K., Taniguchi, T., Manabe, Y., Kaido, M., Mise, K., Sugawara, T., Taniguchi, H., and Okuno, T. (2015) Phosphatidic acid produced by phospholipase D promotes RNA replication of a plant RNA virus. *PLoS Pathog.* **11,** e1004909 CrossRef Medline
33. Xu, K., and Nagy, P. D. (2016) Enrichment of phosphatidylethanolamine in viral replication compartments via co-opting the endosomal Rab5 small GTPase by a positive-strand RNA virus. *PLoS Biol.* **14,** e2000128 CrossRef Medline
34. Sharma, M., Sasvari, Z., and Nagy, P. D. (2011) Inhibition of phospholipid biosynthesis decreases the activity of the tombusvirus replicase and alters the subcellular localization of replication proteins. *Virology* **415,** 141–152 CrossRef Medline
35. Barajas, D., Xu, K., Sharma, M., Wu, C. Y., and Nagy, P. D. (2014) Tombusviruses upregulate phospholipid biosynthesis via interaction between p33 replication protein and yeast lipid sensor proteins during virus replication in yeast. *Virology* **471,** 72–80 CrossRef Medline
36. Li, Z., and Vance, D. E. (2008) Thematic review series: glycerolipids. Phosphatidylcholine and choline homeostasis. *J. Lipid Res.* **49,** 1187–1194 CrossRef Medline
37. Perera, R., Riley, C., Isaac, G., Hopf-Jannasch, A. S., Moore, R. J., Weitz, K. W., Pasa-Tolic, L., Metz, T. O., Adamec, J., and Kuhn, R. J. (2012) Dengue virus infection perturbs lipid homeostasis in infected mosquito cells. *PLoS Pathog.* **8,** e1002584 CrossRef Medline
38. Castorena, K. M., Stapleford, K. A., and Miller, D. J. (2010) Complementary transcriptomic, lipidomic, and targeted functional genetic analyses in cultured *Drosophila* cells highlight the role of glycerophospholipid metabolism in flock house virus RNA replication. *BMC Genomics* **11,** 183 CrossRef Medline
39. Vance, D. E., Trip, E. M., and Paddon, H. B. (1980) Poliovirus increases phosphatidylcholine biosynthesis in HeLa cells by stimulation of the rate-limiting reaction catalyzed by CTP: phosphocholine cytidylyltransferase. *J. Biol. Chem.* **255,** 1064–1069 Medline
40. Banerjee, S., Aponte-Diaz, D., Yeager, C., Sharma, S. D., Ning, G., Oh, H. S., Han, Q., Umeda, M., Hara, Y., Wang, R. Y. L., and Cameron, C. E. (2018) Hijacking of multiple phospholipid biosynthetic pathways and induction of membrane biogenesis by a picornaviral 3CD protein. *PLoS Pathog.* **14,** e1007086 CrossRef Medline
41. Henry, S. A., Kohlwein, S. D., and Carman, G. M. (2012) Metabolism and regulation of glycerolipids in the yeast *Saccharomyces cerevisiae*. *Genetics* **190,** 317–349 CrossRef Medline
42. Summers, E. F., Letts, V. A., McGraw, P., and Henry, S. A. (1988) *Saccharomyces cerevisiae cho2* mutants are deficient in phospholipid methylation and cross-pathway regulation of inositol synthesis. *Genetics* **120,** 909–922 Medline
43. El-Gebali, S., Mistry, J., Bateman, A., Eddy, S. R., Luciani, A., Potter, S. C., Qureshi, M., Richardson, L. J., Salazar, G. A., Smart, A., Sonnhammer, E. L. L., Hirsh, L., Paladin, L., Piovesan, D., Tosatto, S. C. E., *et al.* (2019) The Pfam protein families database in 2019. *Nucleic Acids Res.* **47,** D427–D432 CrossRef Medline
44. Kelley, L. A., Mezulis, S., Yates, C. M., Wass, M. N., and Sternberg, M. J. (2015) The Phyre2 web portal for protein modeling, prediction and analysis. *Nat. Protoc.* **10,** 845–858 CrossRef Medline
45. Shields, D. J., Altarejos, J. Y., Wang, X., Agellon, L. B., and Vance, D. E. (2003) Molecular dissection of the *S*-adenosylmethionine-binding site of phosphatidylethanolamine *N*-methyltransferase. *J. Biol. Chem.* **278,** 35826–35836 CrossRef Medline
46. Ishikawa, M., Janda, M., Krol, M. A., and Ahlquist, P. (1997) *In vivo* DNA expression of functional brome mosaic virus RNA replicons in *Saccharomyces cerevisiae*. *J. Virol.* **71,** 7781–7790 Medline
47. Diaz, A., Wang, X., and Ahlquist, P. (2010) Membrane-shaping host reticulon proteins play crucial roles in viral RNA replication compartment formation and function. *Proc. Natl. Acad. Sci. U.S.A.* **107,** 16291–16296 CrossRef Medline
48. Diaz, A., Zhang, J., Ollwerther, A., Wang, X., and Ahlquist, P. (2015) Host ESCRT proteins are required for bromovirus RNA replication compartment assembly and function. *PLoS Pathog.* **11,** e1004742 CrossRef Medline
49. Li, J., Fuchs, S., Zhang, J., Wellford, S., Schuldiner, M., and Wang, X. (2016) An unrecognized function for COPII components in recruiting a viral replication protein to the perinuclear ER. *J. Cell Sci.* **129,** 3597–3608 CrossRef Medline
50. Kaganovich, D., Kopito, R., and Frydman, J. (2008) Misfolded proteins partition between two distinct quality control compartments. *Nature* **454,** 1088–1095 CrossRef Medline
51. Hardwick, K. G., and Pelham, H. R. (1992) SED5 encodes a 39-kD integral membrane protein required for vesicular transport between the ER and the Golgi complex. *J. Cell Biol.* **119,** 513–521 CrossRef Medline
52. Manford, A. G., Stefan, C. J., Yuan, H. L., Macgurn, J. A., and Emr, S. D. (2012) ER-to-plasma membrane tethering proteins regulate cell signaling and ER morphology. *Dev. Cell* **23,** 1129–1140 CrossRef Medline

53. Schwartz, M., Chen, J., Janda, M., Sullivan, M., den Boon, J., and Ahlquist, P. (2002) A positive-strand RNA virus replication complex parallels form and function of retrovirus capsids. *Mol. Cell* **9,** 505–514 CrossRef Medline
54. Wang, X., Lee, W. M., Watanabe, T., Schwartz, M., Janda, M., and Ahlquist, P. (2005) Brome mosaic virus 1a nucleoside triphosphatase/helicase domain plays crucial roles in recruiting RNA replication templates. *J. Virol.* **79,** 13747–13758 CrossRef Medline
55. Strating, J. R., and van Kuppeveld, F. J. (2017) Viral rewiring of cellular lipid metabolism to create membranous replication compartments. *Curr. Opin. Cell Biol.* **47,** 24–33 CrossRef Medline
56. Stapleford, K. A., and Miller, D. J. (2010) Role of cellular lipids in positive-sense RNA virus replication complex assembly and function. *Viruses* **2,** 1055–1068 CrossRef Medline
57. Romero-Brey, I., and Bartenschlager, R. (2014) Membranous replication factories induced by plus-strand RNA viruses. *Viruses* **6,** 2826–2857 CrossRef Medline
58. Belov, G. A. (2016) Dynamic lipid landscape of picornavirus replication organelles. *Curr. Opin. Virol.* **19,** 1–6 CrossRef Medline
59. Reiss, S., Rebhan, I., Backes, P., Romero-Brey, I., Erfle, H., Matula, P., Kaderali, L., Poenisch, M., Blankenburg, H., Hiet, M.-S., Longerich, T, Diehl, S., Ramirez, F., Balla, T., and Rohr, K. (2011) Recruitment and activation of a lipid kinase by hepatitis C virus NS5A is essential for integrity of the membranous replication compartment. *Cell Host Microbe* **9,** 32–45 CrossRef Medline
60. Borawski, J., Troke, P., Puyang, X., Gibaja, V., Zhao, S., Mickanin, C., Leighton-Davies, J., Wilson, C. J., Myer, V., Cornellataracido, I., Baryza, J., Tallarico, J., Joberty, G., Bantscheff, M., and Schirle, M. (2009) Class III phosphatidylinositol 4-kinase α and β are novel host factor regulators of hepatitis C virus replication. *J. Virol.* **83,** 10058–10074 CrossRef Medline
61. Berger, K. L., Kelly, S. M., Jordan, T. X., Tartell, M. A., and Randall, G. (2011) Hepatitis C virus stimulates the phosphatidylinositol 4-kinase III α-dependent phosphatidylinositol 4-phosphate production that is essential for its replication. *J. Virol.* **85,** 8870–8883 CrossRef Medline
62. Roulin, P. S., Lötzerich, M., Torta, F., Tanner, L. B., van Kuppeveld, F. J., Wenk, M. R., and Greber, U. F. (2014) Rhinovirus uses a phosphatidylinositol 4-phosphate/cholesterol counter-current for the formation of replication compartments at the ER-Golgi interface. *Cell Host Microbe* **16,** 677–690 CrossRef Medline
63. Ilnytska, O., Santiana, M., Hsu, N.-Y., Du, W.-L., Chen, Y.-H., Viktorova, E. G., Belov, G., Brinker, A., Storch, J., Moore, C., Dixon, J. L., and Altan-Bonnet, N. (2013) Enteroviruses harness the cellular endocytic machinery to remodel the host cell cholesterol landscape for effective viral replication. *Cell Host Microbe* **14,** 281–293 CrossRef Medline
64. Rothwell, C., Lebreton, A., Young Ng, C., Lim, J. Y., Liu, W., Vasudevan, S., Labow, M., Gu, F., and Gaither, L. A. (2009) Cholesterol biosynthesis modulation regulates dengue viral replication. *Virology* **389,** 8–19 CrossRef Medline
65. Mackenzie, J. M., Khromykh, A. A., and Parton, R. G. (2007) Cholesterol manipulation by West Nile virus perturbs the cellular immune response. *Cell Host Microbe* **2,** 229–239 CrossRef Medline
66. Xu, K., and Nagy, P. D. (2015) RNA virus replication depends on enrichment of phosphatidylethanolamine at replication sites in subcellular membranes. *Proc. Natl. Acad. Sci. U.S.A.* **112,** E1782–E1791 CrossRef Medline
67. Restrepo-Hartwig, M., and Ahlquist, P. (1999) Brome mosaic virus RNA replication proteins 1a and 2a colocalize and 1a independently localizes on the yeast endoplasmic reticulum. *J. Virol.* **73,** 10303–10309 Medline
68. den Boon, J. A., Chen, J., and Ahlquist, P. (2001) Identification of sequences in brome mosaic virus replicase protein 1a that mediate association with endoplasmic reticulum membranes. *J. Virol.* **75,** 12370–12381 CrossRef Medline
69. Liu, L., Westler, W. M., den Boon, J. A., Wang, X., Diaz, A., Steinberg, H. A., and Ahlquist, P. (2009) An amphipathic α-helix controls multiple roles of brome mosaic virus protein 1a in RNA replication complex assembly and function. *PLoS Pathog.* **5,** e1000351 CrossRef Medline
70. Renne, M. F., and de Kroon, A. I. (2018) The role of phospholipid molecular species in determining the physical properties of yeast membranes. *FEBS Lett.* **592,** 1330–1345 CrossRef Medline
71. Li, Z., Agellon, L. B., Allen, T. M., Umeda, M., Jewell, L., Mason, A., and Vance, D. E. (2006) The ratio of phosphatidylcholine to phosphatidylethanolamine influences membrane integrity and steatohepatitis. *Cell Metab.* **3,** 321–331 CrossRef Medline
72. de Kroon, A. I. (2007) Metabolism of phosphatidylcholine and its implications for lipid acyl chain composition in Saccharomyces cerevisiae. *Biochim. Biophys. Acta* **1771,** 343–352 CrossRef Medline
73. Garcia-Ruiz, H. (2018) Susceptibility genes to plant viruses. *Viruses* **10,** E484CrossRef Medline
74. Matyash, V., Liebisch, G., Kurzchalia, T. V., Shevchenko, A., and Schwudke, D. (2008) Lipid extraction by methyl-tert-butyl ether for high-throughput lipidomics. *J. Lipid Res.* **49,** 1137–1146 CrossRef Medline
75. Castro-Perez, J. M., Kamphorst, J., DeGroot, J., Lafeber, F., Goshawk, J., Yu, K., Shockcor, J. P., Vreeken, R. J., and Hankemeier, T. (2010) Comprehensive LC-MS^E lipidomic analysis using a shotgun approach and its application to biomarker detection and identification in osteoarthritis patients. *J. Proteome Res.* **9,** 2377–2389 CrossRef Medline
76. Zhou, Z., Marepally, S. R., Nune, D. S., Pallakollu, P., Ragan, G., Roth, M. R., Wang, L., Lushington, G. H., Visvanathan, M., and Welti, R. (2011) LipidomeDB data calculation environment: online processing of direct-infusion mass spectral data for lipid profiles. *Lipids* **46,** 879–884 CrossRef Medline
77. Kong, F., Sivakumaran, K., and Kao, C. (1999) The N-terminal half of the brome mosaic virus 1a protein has RNA capping-associated activities: specificity for GTP and S-adenosylmethionine. *Virology* **259,** 200–210 CrossRef Medline

An engineered mutant of a host phospholipid synthesis gene inhibits viral replication without compromising host fitness

Guijuan He, Zhenlu Zhang, Preethi Sathanantham, Xin Zhang, Zujian Wu, Lianhui Xie and Xiaofeng Wang

J. Biol. Chem. 2019, 294:13973-13982.
doi: 10.1074/jbc.RA118.007051 originally published online July 30, 2019
